Investigation of Biomass Ash Sintering Characteristics and the Effect of Additives

ARTICLE *in* ENERGY & FUELS · NOVEMBER 2013

Impact Factor: 2.79 · DOI: 10.1021/ef401521c

4 AUTHORS:

Liang Wang
SINTEF
33 PUBLICATIONS **184** CITATIONS
SEE PROFILE

Geir Skjevrak
Norwegian University of Science and Technol…
11 PUBLICATIONS **116** CITATIONS
SEE PROFILE

Johan E. Hustad
Norwegian University of Science and Technol…
79 PUBLICATIONS **1,611** CITATIONS
SEE PROFILE

Øyvind Skreiberg
SINTEF Energy Research, Trondheim, Norway
76 PUBLICATIONS **831** CITATIONS
SEE PROFILE

energy&fuels

Article

pubs.acs.org/EF

Investigation of Biomass Ash Sintering Characteristics and the Effect of Additives

Liang Wang,*[†,‡] Geir Skjevrak,[†] Johan E. Hustad,[†] and Øyvind Skreiberg[‡]

[†]Department of Energy and Process Engineering, Norwegian University of Science and Technology, NO-7491 Trondheim, Norway

[‡]SINTEF Energy Research, Sem Sælands vei 11, NO-7465 Trondheim, Norway

Supporting Information

ABSTRACT: In this work, the effects of three additives (sewage sludge, marble sludge, and clay sludge) on the sintering behaviors of two types of biomass ash (wheat straw and wood waste ash) were investigated. The ability of the additives to abate sintering was evaluated by performing standard ash fusion characterization and laboratory-scale sintering tests on mixtures of biomass ash and additives. The possible mechanisms underlying the anti-sintering effects of the additives were examined using a combination of X-ray diffraction (XRD) and scanning electron microscopy−energy-dispersive X-ray spectrometry (SEM−EDX) analyses of residues from the sintering tests. The best anti-sintering effect was achieved when marble sludge was used. The diluting effect of the marble sludge on the biomass ashes is considered to be the main reason for the decreased degree of ash sintering. In addition, Ca from the marble sludge may promote the formation of high-temperature melting silicates and phosphates with low K/Ca ratios. These chemical reactions and consequent products are favorable for reducing ash melt formation and sintering tendency. Sewage sludge served as a suitable additive to mitigate the sintering of the studied biomass ashes. Upon addition of the sewage sludge, compositions of the biomass ash changed from low-temperature melting silicates to high-temperature melting silicates, phosphates, and oxides. The shift of ash chemistry had a considerable positive effect on biomass melting and sintering temperatures. Clay sludge exhibited a poor ability to reduce the sintering tendency of wheat straw ash. Moreover, the addition of clay sludge decreased melting temperatures and caused severe sintering behavior of wood waste ash. SEM−EDX and XRD analyses revealed that, as clay sludge was added, more Si-rich melts were formed in wood waste ash. This occurred because clay sludge provides thermodynamically reactive Si-containing species and promotes the formation of low-melting-temperature alkali silicates.

1. INTRODUCTION

Combustion remains the most important technology to generate heat and power from biomass fuels.[1] However, the combustion of biomass fuels is often challenging because of the transformation and interaction of critical ash-forming matters in the fuel.[1,2] Ash-related operational problems, such as sintering and slagging, are frequently encountered in biomass combustion systems.[3−5] Biomass fuels with high sintering tendencies are often rich in potassium, silicon, and phosphorus, and interactions between them play an essential role in the formation of ash melts.[1,6,7] During combustion, potassium in biomass fuels may be involved in complex transformation reactions and partially end up in the form of potassium salts, phosphates, and silicates.[8,9,4,10−13] Some of these potassium-containing compounds and their mixtures have low melting temperatures and occur as viscous melts on the surface of ash/char particles, causing progressive sintering of ash grains. Eventually, the sintered ashes form large size slags that cannot be transformed out of the burner and/or furnace. The ash sintering and slagging decrease the performance of combustion appliances and lead to costly cleaning and maintenance.

One possible method to mitigate biomass ash sintering is to use additives that can increase the ash melting temperature, hinder unwanted reactions, and convert problem species to less troublesome forms.[14,15] Additives with different chemical compositions and physical properties have been investigated for their anti-sintering ability. Aluminum-silicate-based additives, such as kaolin, have been well-studied and exhibit a superior ability to abate biomass ash sintering.[4,16,17] During the combustion of biomass, kaolin can bind potassium-containing species in the form of potassium aluminum silicates.[4] This transformation leads to significant reduction of the amount of formed ash melts and ash sintering degree as well. Calcium-based additives, such as lime and limestone, have been found to be effective in mitigating biomass ash sintering and slag formation.[4,10,18−20] The addition of a calcium-based additive promotes the formation of high-temperature melting calcium-rich silicates and/or phosphates during biomass combustion.[10] In addition, the calcium-based additives give a dilution effect to the biomass ash, restraining physical contact and, hence, sintering of resulting ash particles.[17] Other additives, such as bauxite and silica, have been tested but exhibited poor ability to reduce the sintering of biomass ashes under the tested conditions.[17] The coal and coal ash are also important materials that reduce biomass ash sintering and fouling deposit as stated by previous studies.[21−23] With blending of coal or coal ash, more Al, Si, and Ca will be introduced into the biomass ash. It promotes the formation of high-temperature melting silicates and mitigates

Special Issue: 4th (2013) Sino-Australian Symposium on Advanced Coal and Biomass Utilisation Technologies

Received: August 1, 2013
Revised: November 4, 2013
Published: November 4, 2013

Table 1. Elemental Compositions and Crystalline Phases of Biomass Fuels and Additive Ashes Produced at 550 °C

	wheat straw	wood waste	sewage sludge	clay sludge	marble sludge
ash content (wt %, db)[a]	6.3	0.71	41.7	99	97
Ash Chemical Compositions (wt %, 550 °C)					
SiO_2	39.2	22.75	26.36	60.10	2.00
Al_2O_3	0.90	6.26	31.74	17.10	0.76
CaO	6.10	26.13	13.08	6.40	95.47
K_2O	29.9	14.47	0.69	3.02	0.12
Na_2O	1.10	11.37	0.47	1.50	0.22
P_2O_5	6.26	2.33	16.96	0.20	0.02
Fe_2O_3	0.40	3.56	6.80	2.40	0.57
MgO	1.90	5.77	1.08	8.28	0.79
SO_3	5.03	2.42	1.40	0.06	0.05
Cl	9.2	0.21	0.10	0.01	*b*
TiO_2	0.01	3.08	0.45	0.93	*b*
Crystalline Phases					
major	KCl SiO_2	$CaCO_3$ SiO_2	Al_2O_3 SiO_2	SiO_2 $KAl_2(AlSi_3O_{10})(OH)_2$ $[K(Al,Fe)_2AlSi_3O_{10}(OH)_2{\cdot}H_2O]$	CaO $CaCO_3$ $Ca(OH)_2$
minor	K_2SO_4 $K_2CaP_2O_7$	$CaMg(CO_3)_2$ $NaAlSi_3O_8$ $KAlSi_3O_8$ TiO_2	$(Na_2CaO){\cdot}Al_2O_3{\cdot}2SiO_2$ $CaAl_2Si_2O_8$	$KAlSi_3O_8$ $NaAlSi_3O_8$	$Ca(Fe,Mg)(CO_3)_2$

[a]db = dry basis. [b]Not detected.

ash sintering as a result.[21,23] In addition, sulfur in the coal can also reduce the formation of problematic potassium chloride through different sulfation reactions.[21] This process may also be associated with inhibiting of ash sintering and fouling.

The choice of an appropriate additive is not always straightforward. To minimize the sintering of biomass ash, an additive should ideally be efficient and cheap and have a minor impact on the ash-handling system and environment.[14,24−26] Additives from waste stream resources are of particular interest, which contain active inorganic compounds and are financially attractive. As an example of such additives, sewage sludge derived from the wastewater treatment process has been studied for its ability to reduce biomass ash-related operational problems. Sewage sludge addition promoted the formation of high-melting-temperature potassium silicates and reduced the slag formation during combustion of problematic wood waste in a grate boiler.[27] In a recent study, co-firing sewage sludge with wheat straw significantly impacted bed ash compositions that shift from low-melting-temperature potassium silicates to high-temperature melting phases.[24] The change of ash chemistry resulted in more favorable bed agglomeration characteristics and combustion behavior of the wheat straw. In other studies, sewage sludge mixed with biomass fuels considerably reduce deposit formation on heat-transfer tube surfaces.[28−30] It has been suggested that aluminum silicates, calcium, sulfur, and phosphates provided by the sewage sludge are all involved in the capture of gaseous KCl in flue gas and alleviating deposition during the combustion of such fuels.[29,30] Clay sludge is a slurry waste from sand/clay pits, containing mainly quartz and clay minerals. Clay sludge was used as an additive to reduce fouling deposits in a full-scale wood-chip-fired boiler.[31] In comparison to the combustion of pure wood chips, the rate of ash deposition on a sampling probe placed in the superheater section was considerably decreased upon the addition of clay sludge.[31] The content of KCl in the ash deposit was significantly reduced during these tests, which indicates that KCl has reacted with aluminum silicates present in the clay sludge. Marble sludge is another example of a waste-derived additive that efficiently reduced slag formation during residential wood pellet combustion.[27] The review above suggests that sewage, clay, and marble sludges could be promising for mitigating ash-related operational problems in biomass combustion applications. Only a few studies could be found regarding the ability of these additives to abate sintering of biomass ash, in particular regarding clay and marble sludges. In addition, the mechanisms for the anti-sintering effects of these additives have not been well clarified.

The present work was performed with the aims (1) to characterize sintering behaviors of two problematic fuels, i.e., wheat straw and wood waste, and (2) to investigate anti-sintering effects of the waste-material-derived additives (sewage, marble, and clay sludges) on the two biomass ashes. The anti-sintering mechanisms of the three additives were examined and discussed. The results obtained in this study can provide a better understanding of the sintering behavior of the two tested fuels and valuable information for the selection and optimum application of the three additives in biomass combustion applications.

2. EXPERIMENTAL SECTION

The biomass fuels used in this study were a Danish wheat straw and wood waste. Wheat straw was tested as a representative of largely available agricultural residues, which is often characterized by a high propensity of sintering and slagging in combustion applications. The wood waste used in this study originated from the furniture industry, which is a mixture of processing residues, packing board, panel, etc. The wood waste is currently collected, pelletized, and burned in a grate-fired boiler for heat production. During the combustion of wood waste pellets, ash residues form large aggregates and slags on the grate that cannot be handled by the ash screw and severely influence the combustion process. The boiler has to be shut down frequently for manual cleaning. The sewage sludge used here was obtained as granules from a wastewater processing plant in southern Norway. Clay sludge was obtained as fine particles from a gravel pit. Marble sludge was obtained as slurry waste from a marble processing plant. The received sewage and marble sludges were further air-dried to obtain stable weights.

dx.doi.org/10.1021/ef401521c | Energy Fuels 2014, 28, 208−218

Table 2. Ash Fusion Behaviors of Biomass Ashes with and without Additives

		sewage sludge			marble sludge			clay sludge		
	non-additive	1%	3%	5%	1%	3%	5%	1%	3%	5%
Standard Ash Fusion Tests for Ash from Biomass Fuels and the Corresponding Mixtures with Additives Produced at 550 °C										
Wheat Straw										
initial deformation temperature (IDT, °C)	698	932	990	1004	938	1024	1044	874	924	956
softening temperature (ST, °C)	790	1100	1160	1230	998	1078	1116	926	988	1026
hemisphere temperature (HT, °C)	852	1124	1282	1326	1138	1170	1198	980	1040	1108
flow temperature (FT, °C)	916	1238	1308	1368	1264	1292	1324	1004	1081	1156
Wood Waste										
initial deformation temperature (IDT, °C)	1068	1108	1118	1126	1122	1140	1168	1044	1062	1084
softening temperature (ST, °C)	1152	1166	1206	1240	1258	1280	1322	1138	1148	1176
hemisphere temperature (HT, °C)	1166	1258	1308	1364	1406	1416	1428	1182	1200	1218
flow temperature (FT, °C)	1180	1302	1362	1404	1427	1440	1448	1206	1236	1272

Representative biomass fuels and additive samples were ground to particle sizes less than 1 and 0.1 mm, respectively. According to American Society for Testing and Materials (ASTM) standard D1102, the biomass fuels and additives were ashed at 550 °C for 6 h to determine the ash content. The chemical compositions of the produced ashes were then analyzed using an X-ray fluorescence (XRF) spectrometer. The ash contents and chemical compositions of the fuels and additives are listed in Table 1.

In the experiments, the air-dried additives were first mixed well with ashes obtained from the sample fuels. The amounts of additives corresponded to 1, 3, and 5 wt % of the dry fuels. The amounts of the additives were selected mainly on the basis of two considerations: (1) Results from this work can provide valuable information regarding selection of the appropriate type and amount of additives, which are important for producing biomass pellets with a minimum ash sintering potential. Therefore, the amount of additive should be practically feasible for producing biomass pellets with such additive addition. (2) The ash content of the pellets should not be too high after additive blending, which may cause difficulty for handling and transporting ash residues out of combustion appliances.

Ash fusion and sintering tests were performed to study the anti-sintering effects of the three additives on the two biomass ashes. The fusion temperatures of the reference biomass ashes and the corresponding mixtures with additives were determined according to the ISO 540:1995 standard. Each ash sample was first shaped into a 3×3 mm cubical specimen. The ash specimens were then heated from room temperature to 1500 °C at a heating rate of 6 °C/min in an oxidizing atmosphere in an ash fusion analyzer. On the basis of the shape changes of each ash specimen recorded at elevated temperatures, four ash fusion characteristic temperatures were determined: initial deformation temperature (IDT), softening temperature (ST), hemisphere temperature (HT), and flow temperature (FT). Five tests were performed for each ash sample, and the average test results values are presented in Table 2.

Laboratory sintering tests were performed on two reference fuel ashes prepared at 550 °C and the corresponding mixtures of them with additives. The reference wheat straw ash and the ash−additive mixtures were heated in open crucibles at 700, 800, 900, and 1000 °C for 1 h. The same procedure was performed for the wood waste ash with and without blending of the additives. However, the initial and final sintering test temperatures for the reference wood waste ash and ash-additive mixtures were 800 and 1100 °C, respectively. After heating at the desired temperatures, the sintering behavior of the residues remaining in the crucibles was evaluated on the basis of visual observation of the formed aggregates and slag, as well as the ease of manual disintegration.[17] The sintering degree of the residues was graded according to a scale as follows: (1) loose ash related to residues without any aggregates formation, (2) slightly sintered ash with a fragile structure that is easily broken, (3) hard sintered ash related to partial melting of the residues, (4) very hard sintered ash with the formation of slags difficult to break, and (5) completely melted ash. A similar scale for grading the sintering degree of biomass ash has been used in previous studies.[4]

Ashes produced at 550 °C from the biomass fuels and additives and ash residues collected after the 1000/1100 °C sintering treatment were examined by a Bruker D8 Advance X-ray diffractometer using Cu K-alpha radiation and a LynxEye detector. An instrument-integrated TOPAS evaluation program and the ICDD-PDF2 database were used for processing and identification of the crystalline components. The morphology and microchemistry of the ash residues after the sintering tests were examined by scanning electron microscopy (SEM) combined with energy-dispersive X-ray spectrometry (EDX). Representative ash melts and aggregates were collected and mounted in resin and then cut, ground, and polished to obtain cross-sections with smooth surfaces. The cross-sections were then scanned by a SEM that operated in backscattered electron mode. Semi-quantitative spot analyses were performed using EDX, to obtain element compositions of the samples. Element maps were also obtained to show the distribution of important elements in the sample structure.

3. RESULTS AND DISCUSSION

3.1. Characterization of Fuels and Additives. The chemical compositions and crystalline phases of the ashes from the fuels and additives prepared at 550 °C are presented in Table 1. The wheat straw has a high ash yield at about 6.3% of dry fuel. The dominant elements in the wheat straw ash were Si, K, and Cl, and relatively high contents of Ca, P, and Mg were present. Sylvite (KCl) and quartz (SiO_2) were two of the main crystalline phases identified in the reference wheat straw ash (550 °C). Small amounts of K_2SO_4 and $K_2CaP_2O_7$ were also observed. The ash content of the wood waste is 0.71% of the dry fuel. However, high contents of K and Na (in oxide form) were detected in the reference wood waste ash (550 °C), accounting for about 14.47 and 11.37% of the dry ash. The other main elements in the wood waste ash are Si, Ca, and Fe. The element Ti detected in the wood waste ash is possibly a remaining component from paint. Calcite ($CaCO_3$) and quartz (SiO_2) were identified as the main crystalline phases in the reference wood waste ash. In addition, minor amounts of potassium feldspars ($KAlSi_3O_8$) and albite feldspars ($NaAlSi_3O_8$) were also observed in the wood waste ash (550 °C). The studied sewage sludge has a high ash yield that is 41.7% of the dry matter, which is dominated by the ash-forming elements Al, Si, P, and Ca. The high Al content is mainly due to the use of the precipitation agent $Al_2(SO_4)_3$ for binding phosphorus during the sludge-conditioning stage. Aluminum oxide from the decomposition of $Al_2(SO_4)_3$ during the ashing process was identified as corundum by the XRD analysis. The crystalline phase $(Na_2CaO)\cdot Al_2O_3\cdot 2SiO_2$ most likely arose from the presence of zeolites that mainly comprise aluminum silicates with various Si/Al molar ratios. Zeolites are an important component of washing detergents that are captured in

dx.doi.org/10.1021/ef401521c | Energy Fuels 2014, 28, 208−218

wastewater and largely end up in sewage sludge.[28,29] As shown in Table 1, clay and marble sludges contain mainly incombustible material. Clay sludge ash contains significantly high concentrations of Si and Al. XRD analysis showed that the clay sludge used is a mixture of quartz and various aluminum silicates. Marble sludge is almost pure CaO, but minor amounts of SiO_2, MgO, and Al_2O_3 are present.

3.2. Melting and Sintering of Biomass Ash. The ash melting temperatures of the two reference biomass ashes are listed in Table 1. The ash fusibility test characterizes the temperatures at which the various stages of ash softening, melting, and flowing occur.[33] The determination of the initial deformation temperature (IDT) is of particular concern because ashes from solid fuels usually become sticky and easily sinter at this temperature. The wheat straw ash started to melt at approximately 700 °C and was completely fused at 916 °C. Swelling and shrinking of the ash cubic specimens were clearly observed during the fusion test, which indicates that they passed through a severely molten stage. After the ash fusion test, transparent glassy deposits remained on the sample holder surface, representing complete melting of the ash sample with the depletion of the solid materials. Melting of wood waste ash commenced at 1068 °C, and the ash was completely melted within a short time at 1180 °C. As shown in Figure 1, the results

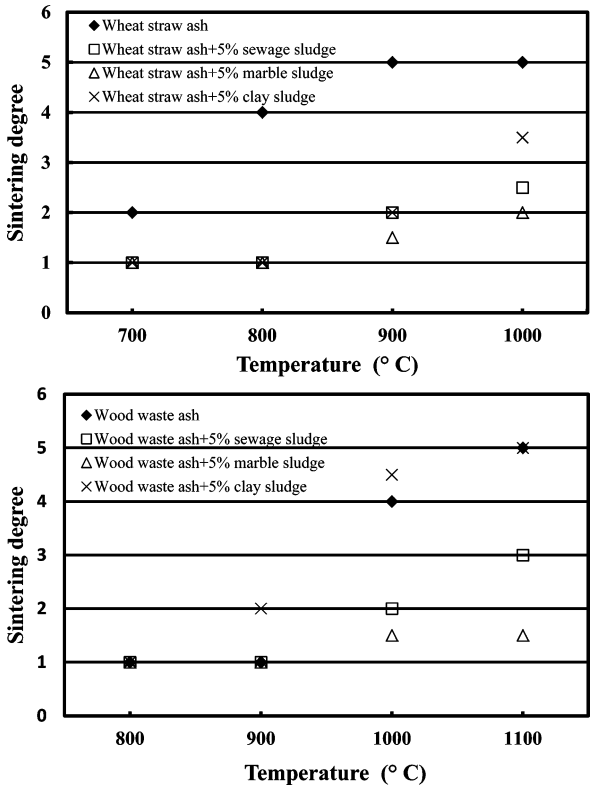

Figure 1. Sintering behavior of biomass ashes and the effects of additives.

of the sintering evaluation of the biomass ashes were consistent with the results of the ash fusion test. The wheat straw ash was already hard-sintered at 800 °C and completely melted at 900 °C. Part of the ash residues shrank and formed greenish droplets on the bottom of the crucibles.

XRD analysis has been proven useful for studying the biomass ash chemistry and transformation of important ash-forming matters. However, one weakness of this technique should be noted. Material that exists in amorphous phases in an ash sample cannot be directly identified and is seen in the diffraction spectrum as a broad hump on the baseline.[16] The amorphous materials are often related to the melted fractions in the biomass ash. It is necessary to obtain more information about these amorphous phases to clarify the underlying ash sintering mechanisms. Therefore, SEM−EDX analyses were performed for representative samples to provide supplementary microchemistry information.

As shown in Table 3, no evident crystalline phases were identified in the wheat straw ash sintered at 1000 °C. The wheat straw ash contained mainly amorphous phases that presented as a broad peak in the XRD spectrum (data not shown).[14] In comparison to crystalline phases observed in the reference wheat straw ash (550 °C), significant depletion of K-bearing salts was observed for the wheat straw ash sintered at 1000 °C. This finding is consistent with previous studies reporting sublimation of KCl and K_2SO_4 from the wheat straw ash at elevated temperatures.[34,35] Figure 2a presents a typical SEM image of cross-sectioned wheat straw ash slag showing hollow bubbles in a continuous and glassy phase. One area, which is marked with a white rectangle in Figure 2b, was examined at a higher magnification. EDX spot analyses (spots 1 and 2 in Table 4) revealed that melted wheat straw ash mainly contain elements K and Si that show clear correlations in the elemental maps (see Figure S1 of the Supporting Information). It manifests that the formation of potassium silicates plays a critical role during sintering of wheat straw ash, as reported by other studies.[3,4] High contents of K and P and minor amounts of Ca were detected in the zones with light gray color (spots 3 and 4 in Table 4), which can easily be distinguished in the elemental maps. Therefore, these zones possibly represent melted potassium-rich phosphates, which also contributed to melt formation in the wheat straw ash. The dark gray zone represents a soil particle trapped by the melted ash, in which Si is detected as a main element (spot 5 in Table 4). As stated in many previous studies, the severe sintering of wheat straw ash is mainly due to the formation and melting of potassium salts, potassium silicates, and potassium-rich phosphates at elevated temperatures.[3−10] In this work, identification of high concentrations of K, Si, Cl, and S as well as a combination of XRD and SEM−EDX analyses of the wheat straw ash all confirm the results reported in the previous studies.

The wood waste ash retained a rather loose structure until the temperature reached 900 °C. After heating at 1000 °C for 1 h, the wood waste ash was hard-sintered and contained visible ash melts and aggregates. When heated at 1100 °C, the wood waste ash fused completely on the bottom of the crucibles. In the fused wood waste ash, $CaTiO_3$ and $Ca_3Mg(SiO_4)_2$ were the two main crystalline phases identified by XRD. A small amount of CaO was also observed. XRD analysis also indicated the appearance of a significant amount of amorphous phase in the wood waste ash (1100 °C). SEM analysis (Figure 3) revealed that the wood waste ash melted into a continuous phase after heating at 1100 °C. The rectangular area marked in Figure 3a was selected for micromorphology and microchemistry analyses. Notable contents of K and Na (>20 wt %) were detected in gray and dark zones (sampling spots 1−4), which showed clear correlation in element mapping (see Figure S5 of the Supporting Information). Considering that high contents of K and Na were detected by SEM−EDX (spots 1−4) in comparison to the amounts of K-/Na-bearing crystalline phases in the wood waste ash (1100 °C) identified by XRD, there are evident deficiencies of K and Na in

dx.doi.org/10.1021/ef401521c | Energy Fuels 2014, 28, 208−218

Table 3. Crystalline phases identified in wheat straw ash with additives sintered at 1000 °C and wood waste ash with additives sintered at 1100 °C

			sewage sludge			marble sludge			clay sludge		
		non-additive	1%	3%	5%	1%	3%	5%	1%	3%	5%
wheat straw	major			Al_2O_3 $KAlSi_2O_6$ $KCa_9Mg(PO_4)_7$ $K_2Ca(SiO_4)_2$	Al_2O_3 SiO_2 $KCa_9Mg(PO_4)_7$ $CaAl_2Si_2O_8$	$CaSiO_3$ $Ca_3Si_2O_7$ $K_2Ca(SiO_4)_2$ $Ca_{10}K(PO_4)_7$	CaO $Ca(OH)_2$ $CaSiO_3$ $Ca_3Si_2O_7$	CaO $Ca(OH)_2$	SiO_2	SiO_2 $KAlSi_3O_8$	SiO_2 $KAlSi_3O_8$ $CaAl_2Si_2O_8$ $MgAl_2SiO_3O_{10}$
	minor		Al_2O_3 $KAlSi_2O_6$ $Ca_{10}K(PO_4)_7$ $CaKPO_4$	SiO_2 $CaKPO_4$ $CaSiO_3$	$CaMg(CO_3)_2$ $Ca_{19}Fe_2(PO_4)_{14}$ $KAlSi_3O_8$	$KCaPO_4$	Ca_2SiO_4 $K_2Ca(SiO_4)_2$ MgO $Ca_{10}K(PO_4)_7$	Ca_2SiO_4 $Ca_3Si_2O_7$	$KAlSi_2O_6$ $K_2Mg(SiO_4)_2$ $KAlSiO_4$	$KAlSi_2O_6$	$KAlSi_2O_6$
wood waste	major	$CaTiO_3$ $Ca_3Mg(SiO_4)_2$	$CaTiO_3$ $Ca_2Al_2SiO_7$ $K_2Ca(SiO_4)_2$	Al_2O_3 $Ca_2Al_2SiO_7$ $KCa_9Mg(PO_4)_7$ $CaSiO_3$ $Ca_7Mg_2P_6O_{24}$	Al_2O_3 SiO_2 $Ca_2Al_2SiO_7$ $KCa_9Mg(PO_4)_7$ $CaAl_2Si_2O_8$ $CaSiO_3$	CaO $CaTiO_3$	CaO $Ca(OH)_2$	CaO $Ca(OH)_2$ $CaCO_3$			
	minor		Al_2O_3 $KAlSi_2O_6$ $Na_2Al_2Si_2O_8$	SiO_2 $KAlSi_2O_6$	$CaMg(CO_3)_2$	$Ca(OH)_2$ $CaSiO_3$ $Ca_3Mg(SiO_4)_2$ $K_4CaSi_3O_9$	Ca_2SiO_4 MgO $Ca_2Al_2SiO_7$ $CaCO_3$	MgO Ca_2SiO_4	$Ca_3Mg(SiO_4)_2$ $Ca_2Al_2SiO_7$	$Ca_3Mg(SiO_4)_2$	

dx.doi.org/10.1021/ef401521c | *Energy Fuels* 2014, 28, 208−218

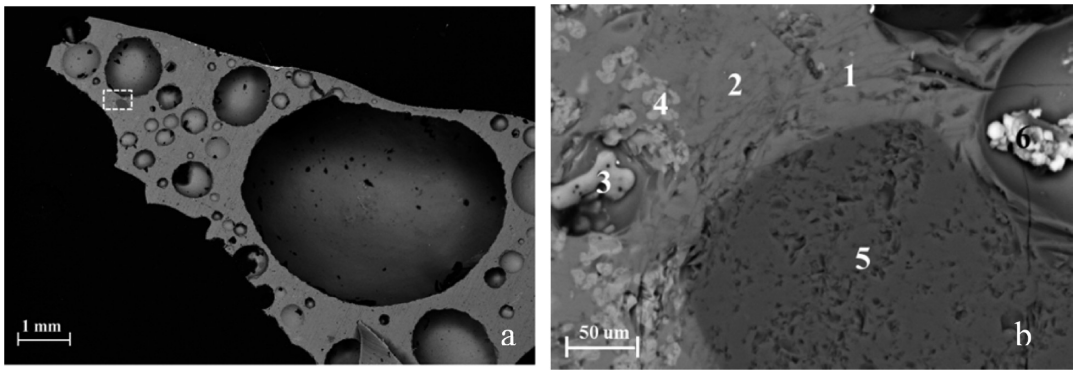

Figure 2. (a) SEM image of wheat straw ash melted at 1000 °C. (b) SEM image of the selected area marked in panel a.

the latter. The deficiency may be explained by the formation of amorphous materials containing K and Na, which are not detectable by XRD. SEM−EDX revealed that the overall compositional distributions of the wood waste ash melt are limited to various $K_2O/Na_2O-Al_2O_3-SiO_2$ (spots 1 and 2 in Figure 3b) and $K_2O/Na_2O-CaO-SiO_2$ (spots 3 and 4 in Figure 3b) ternary systems. Extraction of data from the two silicate phase diagrams indicated that the melting temperatures of silicates with similar elemental distributions detected in spots 1−4 were less than 1000 °C.[36] The formation of silicates was also supported by the finding of strong correlations among K, Na, Si, Al, and Ca, as shown on the element maps (see Figure S5 of the Supporting Information). It suggests that wood waste ash heating at 1100 °C contains mainly silicate melts. Together with the investigation of element concentrations in the dry fuel, results of SEM−EDX and XRD analyses on the wood waste ash agree well with other relevant studies that (1) the sintering tendency of woody biomasses correlates well with concentrations of alkali metals and Si in the fuel and (2) alkali silicate chemistry plays a critical role in initiating and promoting ash sintering.[6,7,10,19] High Ca and Ti contents (>95%) were detected in the round grain containing spot 6, which show clear correlation in element maps. This grain represents the formation of $CaTiO_3$ in the wood waste ash (1100 °C). Ca−Mg silicates were also formed, as revealed by EDX analysis (spot 5 in Figure 3a).

3.3. Anti-sintering Effects and Possible Mechanism of Sewage Sludge. As shown in Table 2, the initial fusion temperature of the wheat straw ash distinctly increased more than 200 °C with the addition of sewage sludge. The evident melting of the wheat straw ash was significantly reduced when sewage sludge was added. Upon heating at 1000 °C, the major portion of the wheat straw ash−sewage sludge mixture was slightly sintered with a fragile structure. At the same time, partially melted ash was also clearly observed. Therefore, the sintering degree of the residue from the wheat straw ash−sewage sludge mixture was graded with degree 2.5, which indicates the coexistence of slight and hard-sintered ash fractions. Minor amounts of $KAlSi_2O_6$, Al_2O_3, $Ca_{10}K(PO_4)_7$, and $CaKPO_4$ were identified in the residues remaining from the wheat straw ash with 1% sewage sludge sintered at 1000 °C (Table 3). Observation of $KAlSi_2O_6$ is possibly due to reactions of aluminum silicates in sewage sludge (i.e., zeolites) with potassium-containing compounds in wheat straw ash.[3,32] The amount of $KAlSi_2O_6$ considerably increased upon 3% sewage sludge addition. Adding sewage sludge also led to the formation of $Ca_{10}K(PO_4)_7$ and $CaKPO_4$. It has been stated that potassium has a high affinity for the reaction with phosphorus to form K phosphates during biomass combustion.[13,37] As encountered with calcium oxide, further reactions may take place with the formation of K−Ca phosphates consequently.[7] Therefore, identification of the two phosphates suggest that phosphorus and calcium in the sewage sludge act favorably to immobilize K into more stable ternary phosphate structures. A large amount of corundum (Al_2O_3) was identified in the residues from the wheat straw ash−sewage sludge mixtures, which has a melting point higher than 2000 °C.[38] When 5% sewage sludge was added, corundum (Al_2O_3) and quartz (SiO_2) were the two main crystalline phases identified in the resulting ash residues. Figure 4a presents a SEM image of an aggregate collected from the sintered residues of wheat straw ash with 1% sewage sludge addition. Chemical compositions in the light gray zone analysis (spots 1 and 2 in Table 5) are similar as those detected from the reference wheat straw ash (spots 1 and 2 in Figure 2b and Table 4). Therefore, the light gray zone represents the fraction of the wheat straw ash melted during sintering of the ash−sewage sludge mixture, with a hollow bubble and continuous phase. A large grain in the left corner of Figure 4a is bonded to the melted ash. Al and Si were detected as two dominant elements in spot 3 (Table 5), which exhibit strong correlations in the element maps (see Figure S2 of the Supporting Information). Thus, the EDX analysis results suggest that the grain consists of aluminum silicates. In comparison to sampling spot 3 in the middle of the large grain, the location of spot 4 is much closer to melted ash, representing the initial formation of the neck. The concentrations of K and Si at spot 4 are higher than those detected at spot 3. In addition, the ratio of the molar concentration of K, Si, and Al at spot 4 is about 1:2:1 and close to that of leucite $KAlSi_2O_6$. Therefore, the composition of spot 4 at the neck implies the presence of potassium aluminum silicates, which is consistent with XRD analysis results shown in Table 3. One large grain (spot 5) and several small grains (spot 6) in dark gray colors were attached to or embedded within the molten ash. The high Al, P, and Ca contents of these grains therefore suggest that they are fine sewage sludge particles trapped in melted wheat straw ash.

The addition of sewage sludge prevented sintering of wood waste ash in the whole temperature range tested. Part of the ash residues from the mixture of wood waste ash and sewage sludge obtained at 1100 °C bonded weakly, and the aggregates were easily crushed. Silicates with high melting temperatures were identified in the ash residues, resulting from heating of the mixture of wood waste ash and 1% sewage sludge at 1100 °C, including $Ca_2Al_2SiO_7$ (1593 °C), $K_2Ca(SiO_4)_2$ (1600 °C), $KAlSi_2O_6$ (1500 °C), and $Na_2Al_2Si_2O_8$ (1250 °C).[17,36] In addition, the amount of amorphous phase in the resultant ash residues was evidently lower than that in the original wood waste

dx.doi.org/10.1021/ef401521c | Energy Fuels 2014, 28, 208−218

Table 4. EDX Spot Analysis Results Referring to Figures 2 and 3

	wheat straw ash						+1% sewage sludge						+1% marble sludge						+1% clay sludge					
	spot																							
(wt %)	1	2	3	4	5	6	1	2	3	4	5	6	1	2	3	4	5	6	1	2	3	4	5	6	7
K	41	38	48	45	1	54	36	33	12	24	3	13	25	27	8	6	25	21	22	1	1	11	12	22	52
Si	51	53	1	1	97	0	45	46	9	39	39	41	49	43	34	38	3	1	55	98	97	53	49	46	0
Ca	2	2	13	17	0	0	7	6	7	5	9	9	16	23	50	52	44	47	9	0	0	1	2	4	0
P	2	2	37	34	1	0	6	7	3	7	7	11	3	2	4	1	27	30	0	0	1	1	1	1	1
Na	0	0	0	1	0	0	1	1	0	0	8	4	2	1	2	1	0	0	1	0	0	2	3	1	0
Mg	1	2	1	1	0	0	3	1	1	0	1	1	3	3	1	1	0	2	4	0	0	0	2	0	0
Al	1	1	0	1	1	0	1	5	37	18	34	20	2	2	1	1	0	0	8	1	1	33	31	26	0
S	1	2	0	0	0	0	0	0	1	1	0	0	0	0	0	0	0	0	0	0	0	0	0	0	0
Cl	0	0	0	0	0	45	0	0	0	0	0	0	1	0	0	0	0	0	0	0	0	0	0	0	46

ash heated at the same temperature. As discussed above, the severe fusion of the wood waste ash is caused by the formation and melting of low-temperature-melting alkali silicates. Aluminum silicates from sewage sludge may react with melted alkali silicates to promote the formation of high-temperature-melting alkali aluminum silicates. The observed $KAlSi_2O_6$ and $Na_2Al_2Si_2O_8$ are probably products from these crystalline reactions. This process was accompanied by reduction of ash melt formation and sintering degree. As for the wheat straw case, corundum (Al_2O_3) and quartz (SiO_2) became dominant mineral phases in resulting ash residues from the wood waste−additive mixture. In addition, new phosphates and the Ca-bearing silicates $CaSiO_3$ and $CaAl_2Si_2O_8$ were identified. All of these new phases are inert at high temperatures and may contribute to the low sintering degree of the ash residues.

3.4. Anti-sintering Effects and Possible Mechanism of Marble Sludge. The addition of marble sludge significantly enhanced the initial fusion temperature of the wheat straw ash but gave a less pronounced effect on that of the wood waste ash. As shown in Figure 1, the addition of marble sludge effectively mitigated the sintering of the studied biomass ashes. After sintering tests, the major fraction of the ash−marble sludge mixtures resembled the original loose structure without observing bridging and agglomeration of ash grains. The addition of 1% marble sludge mainly introduced calcium into the wheat straw ash, and the mineral phases $CaSiO_3$, $Ca_3Si_2O_7$, and $K_2Ca(SiO_4)_2$ emerged in the resulting ash, as shown in Table 3. As higher doses of marble sludge were added to the wheat straw ash, large amounts of CaO and $Ca(OH)_2$ were identified in the wheat straw ash−marble sludge mixtures after heating at 1000 °C . The observation of CaO and $Ca(OH)_2$ indicates the presence of a surplus of added marble sludge, which diluted the wheat straw ash. Figure 4b shows a representative SEM image of a slag sample collected from the wheat straw ash and 1% marble sludge mixture. Two zones can be clearly distinguished on the basis of their different brightnesses. The dark gray areas with a continuous phase represent the molten portion of the resultant ash residues, in which K, Si, and Ca are the main elements detected (spots 1 and 2 in Table 5). The EDX analysis results imply the formation of K−Ca silicates during the heating of the wheat straw ash−marble sludge mixture. Several discrete light gray grains are displayed in Figure 4b, which can be clearly seen in element mapping (see Figure S3 of the Supporting Information). The needle-shaped ash grains (spots 3 and 4 in Table 5) are Si−Ca rich (>95 wt %), representing the formation of Ca silicates in the resulting ash. The EDX analysis results are consistent with XRD analysis in that Ca silicates and K−Ca silicates were major crystalline phases observed in wheat straw ash−marble sludge mixtures. As discussed above, the sintering of wheat straw ash is mainly due to the formation of potassium silicate melt. The calcium oxide from marble sludge may react with potassium silicates and dissolve in the melt. This process will enhance the formation of high-temperature melting Ca silicates and Ca−K silicates and decrease the amount of ash melt formed.[39] In spots 5 and 6, Ca and P were the main elements detected and minor amounts of K were also present. Together with XRD analysis results, the grains containing spots 5 and 6 related to the formation of phosphates with high Ca/K ratios. A similar ash transformation chemistry has been observed for a wheat straw ash heated with limestone addition.[4,10]

The addition of marble sludge eliminated the sintering of wood waste ash in all of the sintering tests. The mineral phases CaO and $Ca(OH)_2$ were identified in the wood waste ash−

dx.doi.org/10.1021/ef401521c | Energy Fuels 2014, 28, 208−218

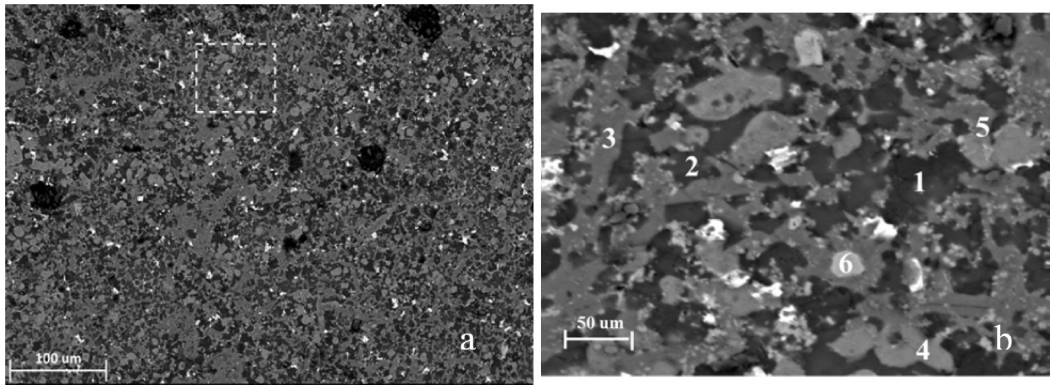

Figure 3. (a) SEM image of wood waste ash melted at 1100 °C, (b) SEM−EDX analyses of the area selected in panel a.

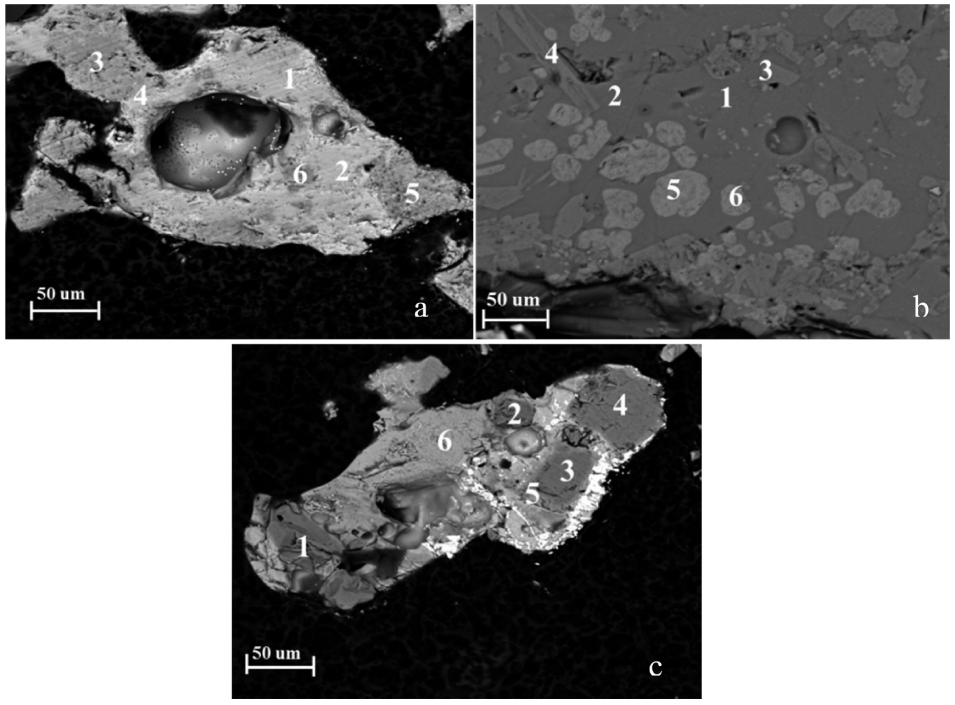

Figure 4. SEM−EDX analyses of slag collected from mixtures of wheat straw ash with the addition of (a) 1% sewage sludge, (b) 1% marble sludge, and (c) 1% clay sludge sintered at 1000 °C.

Table 5. EDX Spot Analysis Results Referring to Figures 4 and 5

	wood waste ash						+1% clay sludge						+3% clay sludge					+5% clay sludge				
	spot																					
(wt %)	1	2	3	4	5	6	1	2	3	4	5	6	1	2	3	4	5	1	2	3	4	5
K	22	19	14	13	7	0	14	15	5	5	19	16	6	7	9	8	11	7	5	8	5	2
Si	26	27	35	31	34	2	30	27	30	32	28	31	33	30	40	37	39	35	39	39	40	41
Ca	1	1	22	25	39	45	38	40	40	39	11	13	36	39	28	29	30	24	23	27	29	33
P	0	1	1	1	2	0	2	2	1	1	4	1	0	1	1	1	0	1	1	2	0	0
Na	22	21	19	20	5	1	7	8	4	3	16	16	7	5	10	13	9	13	11	8	8	1
Mg	2	1	6	5	9	1	3	3	11	13	4	4	14	15	3	2	1	4	4	2	12	10
Al	25	29	2	3	3	0	5	4	8	5	17	19	3	2	6	8	9	14	12	11	6	4
Ti	1	0	0	2	3	51	2	1	2	1	3	2	1	1	3	2	0	1	2	4	0	0

marble sludge mixture after heating at 1100 °C. A similar diluting effect of calcium-rich additives on biomass ashes has been reported in previous studies and is considered to be the main anti-sintering mechanism of calcium-based additives.[17] Upon marble sludge addition, the general wood waste ash composition was changed with enhancement of Ca. Elemental calcium and/or calcium in oxide form may dissolve in potassium silicate melts and drive potassium out of the melt, with a reduction of the amount of melt formed as a result.[7] Global equilibrium calculation results showed that, by increasing the Ca content,

dx.doi.org/10.1021/ef401521c | *Energy Fuels* 2014, 28, 208−218

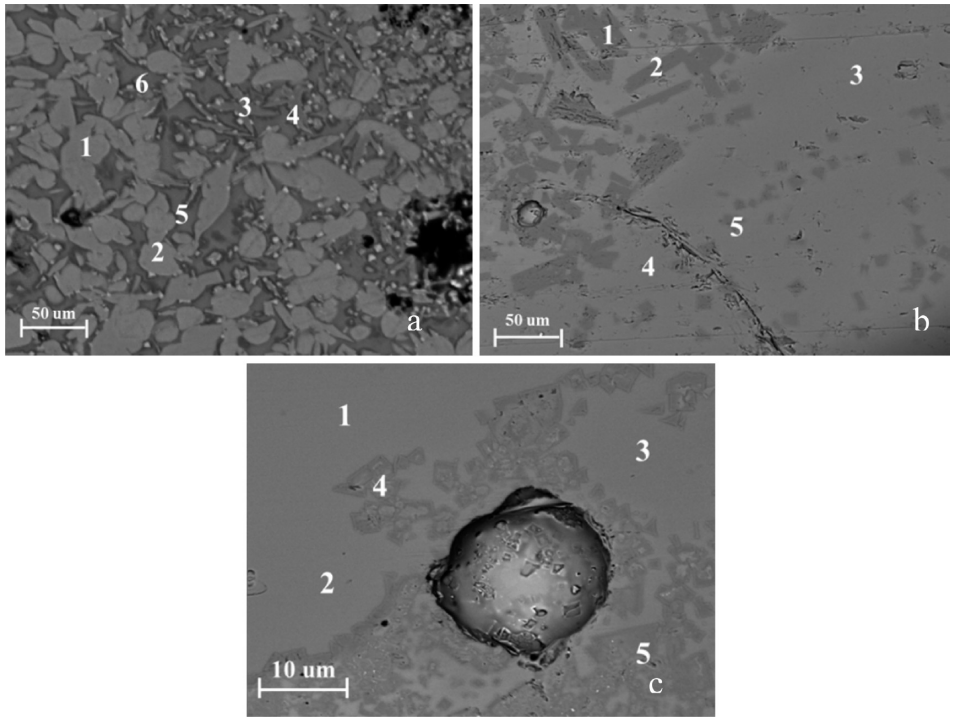

Figure 5. SEM−EDX analyses of slag collected from the mixtures of wood waste ash and (a) 1% clay sludge, (b) 3% clay sludge, and (c) 5% clay sludge sintered at 1100 °C.

the formation of potassium silicates can be reduced and even be completely eliminated during thermal conversion of biomass fuels in the temperature interval of 700−950 °C.[40] Therefore, the formation of low-melting-temperature alkali silicates can be restricted in wood waste ash by the addition of marble sludge. This assumption was supported by the observation of Ca silicates and the lack of alkali silicates in the resultant ash.

3.5. Anti-sintering Effects and Possible Mechanism of Clay Sludge. The melting temperature of the wheat straw ash rose with the addition of clay sludge, as shown in Table 2. However, in comparison to the other two additives, clay sludge gave less pronounced increasing effects on the wheat straw ash fusion characteristic temperatures. After heating treatment, the mixture of wheat straw ash and clay sludge was sintered at 900 °C and was partially melted after heating at 1000 °C. Upon clay sludge addition, silica in the form of quartz and tridymite were identified from the wheat straw ash. It should be noted that several potassium aluminum silicates were also observed. As shown in Table 1, clay sludge contains the silicates muscovite and illite. These two mineral phases may decompose into simpler aluminum silicates at elevated temperatures and react with potassium-containing compounds in the wheat straw ash. $KAlSiO_4$ and $KAlSi_2O_6$ are probably products from such reactions, as indicated by XRD analysis results. Considering high melting points of these potassium aluminum silicates, the formation of them can result in improvement of the sintering behavior of wheat straw ash. Figure 4c shows clear fusion of the mixture of wheat straw ash with 1% clay sludge. The light gray areas are the molten fraction of the wheat straw ash and exhibit a continuous phase. The two small grains (spots 1 and 2 in Figure 4c and Table 5) consisted of nearly pure Si (>97 wt %) and represent inert soil/sand grains embedded in the melted ash. Si, Al, and K were the main elements present in the two larger grains (spots 3 and 4) and showed strong correlations in the element map (see Figure S4 of the Supporting Information). Therefore, the two ash grains possibly contained potassium aluminum silicates as identified by the XRD.

The sintering test results showed that the melted fractions increased markedly when clay sludge was added to wood waste ash. The resulting ash residues from mixtures of wood waste ash and clay sludge contained large amounts of amorphous materials. Only trace amounts of $Ca_3Mg(SiO_4)_2$ and $Ca_2Al_2SiO_7$ were observed. As shown in Table 3, alkali feldspars ($KAlSi_3O_8$ and $NaAlSi_3O_8$) were observed in wood waste ash treated at 550 °C, and these minerals may melt at 1100 °C.[40] Upon the addition of clay sludge, the content of quartz in the wood waste ash was significantly enhanced. The quartz may react with alkali feldspars in the wood waste ash to form a melt that is rich in silica.[41] In addition, as indicated by SEM−EDX and XRD analyses, alkali−calcium silicates were most likely formed during heating of the wood waste ash at 1100 °C. The melting temperature for Si-rich alkali calcium silicates can be as low as 720 °C.[41,43] Increased Si concentrations arising from the addition of clay sludge may enhance the formation of Si-rich alkali calcium silicates and decrease the melting temperature of the resultant ash. This finding agrees well with results from a previous study, where the slagging of wood pellet ash was aggravated because of the contamination of sand minerals.[41] The other main component of clay sludge, illite, has a relatively high fusion temperature of approximately 1200 °C. However, during the sintering test, the reactions between illite, feldspar and quartz in the wood waste ash-clay sludge mixture may occur with formation of different silicates as a result.[44] Part of these silicates may fuse already at 900 °C, which increases the melted fraction in the resultant ash consequently. Figure 5a shows a typical SEM image of melted wood waste ash with 1% clay sludge addition. On the basis of EDX spot analyses, the lighter gray zones (spots 1 and 2 in Figure 5a) indicate the presence of K/Na−Ca silicates. Strong correlations among the four elements K, Na, Si, and Ca are shown in the elemental maps (see Figure S6 of the Supporting

dx.doi.org/10.1021/ef401521c | *Energy Fuels* 2014, 28, 208−218

Information). Some of these light gray zones are connected with each other, which represents the melting and intergrowth of K/Na−Ca-silicate-rich grains into larger grains. Branch-like zones can also be distinguished in Figure 5a, which represent Ca−Mg silicates, as indicated by EDX analyses (spots 3 and 4 in Figure 5a). The interstitial areas (spots 5 and 6 in Figure 5a) between the two types of zones are rich in K, Na, Al, and Si and are in a homogeneous phase that are quenched melts containing alkali−aluminum silicates. Panels b and c of Figure 5 show typical images of sintered products and depict the more severe melting of wood waste ash that occurred with the addition of increasing amounts of clay sludge. Only two zones with different brightnesses can be distinguished in Figure 5b. EDX spot analyses revealed that the dominant, light gray zone (spots 3 and 4 in Figure 5b) represents melted Si-rich K/Na−Ca silicates. The rectangular and irregularly shaped zones (spots 1, 2, and 5 in Figure 5b) are related to the formation of unfused Ca−Mg silicates that were embedded in the melted phase. As shown in element maps (see Figure S7 of the Supporting Information), calcium was clearly correlated with magnesium and silicon, confirming the presence of Ca−Mg silicates in these zones. The addition of 5% clay sludge further increased the melting degree of wood waste ash, which has a more homogeneous structure as shown in Figure 5c. Similar to Figure 5c, the continuous light gray areas represent the formation of Si-rich alkali−calcium silicates, as indicated by EDX spot and mapping examination. EDX spot (spots 4 and 5 in Figure 5c) and elemental mapping analyses (see Figure S8 of the Supporting Information) revealed that the small dark gray patches represent Ca−Mg silicates. As displayed in Figure 5c, these Ca−Mg-silicate-rich zones are connected with each other and form more continuous phases, indicating gradual transition and melting of the Ca−Mg silicates along with the addition of more clay sludge in the wood waste ash. A decrease in the amount of crystalline Ca−Mg silicates has been observed in the ash residues produced during woody biomass combustion with sand contamination.[41] This occurred as a result of complex interaction, assemblage, and transition of the mineral phases. Altogether, the addition of clay sludge provides thermodynamically active Si-rich species (i.e., quartz, alkali feldspar, and illite) that may react with wood waste ash melts and result in the further formation of low-temperature melting silicates. The ratio between the glass and crystalline phases in the wood waste ash increased consequently. This partially explains intensive melting of mixtures of wood waste ash upon clay sludge addition and the disappearance of crystalline phases in the sintered products.

4. CONCLUSIONS AND COMMENTS

Severe sintering behaviors of wheat straw and wood waste ashes were observed in this study. Analysis results revealed that the wheat straw ash melted because of the formation of low-temperature melting potassium silicates and potassium phosphates with a high K/Ca ratio at elevated temperatures. The severe sintering of the wood waste ash was mainly associated with the formation of K/Na−Al silicates and K/Na−Ca silicates with low melting points.

The three additives, i.e., sewage, marble, and clay sludges, were applied to reduce the sintering of the two studied biomass ashes. Marble sludge was the most efficient additive in terms of eliminating the sintering of the biomass ashes, even when the amount added was small. The dilution of the biomass ashes by the marble sludge was considered to be the main reason for the improvement in ash sintering behavior. The calcium present in the marble sludge may also promote the formation of high-temperature melting Ca silicates and K−Ca phosphates, thereby increasing the sintering temperature of the biomass ashes. Sewage sludge exhibited the ability to reduce the degree of sintering of both biomass ashes. The addition of sewage sludge enhanced the formation of refractory mineral phases in biomass ashes, which resulted in higher melting temperatures and reduced the sintering tendency of the two ashes. In addition, SEM−EDX and XRD analyses also indicate that reactions occurred between aluminum silicates contained in the sewage sludge and alkali-containing species in the biomass ashes. Clay sludge exhibited a poor ability to abate the sintering of wheat straw ash. The addition of clay sludge particularly enhanced the sintering of wood waste ash with the consequent formation of a larger proportion of melted ash. For this reason, clay sludge is not recommended as an additive for reducing the sintering tendency of biomass ashes with high alkali content.

Use of additives has been proven efficient to abate ash-related operational problems in different biomass combustion applications. In light of available experimental studies and industrial-scale tests, an optimal additive is generally characterized with (1) high reactivity and capacity to reduce the amount of problematic compounds (i.e., alkali chloride) irreversibly in a combustor, (2) low costs for use and a large amount available, and (3) minimum effects on the ash-handling system.[14,25] The proper blending ratio of one additive to the fuel depends upon a number of factors. First, the amount of additive blended should be sufficient for the expected reactions and cause significant mitigation of the ash-related operational problems. On the other hand, the blending of a certain amount of additive to one fuel should be practically feasible.[4] This is more evident for producing biomass pellets with additive addition, considering the power consumption for pellet production, performance of the pelletizer, and quality of the produced pellets. In previous studies, additives have been added to different problematic fuels with an additive/fuel blending ratio less than 5% (w/w) of dry fuel.[27,42] In addition, the possible blending ratio of additive/fuel is influenced by flexibility of the applied combustion technology and/or appliance. For example, residential pellet combustion appliances are more sensitive to the amount of ash residues remaining on the grate. Therefore, the addition of large amounts of additive may increase the ash-slagging tendency and give negative effects on the combustion process as a result. On the contrary, a high blending ratio of up to 10% (w/w) additive/dry fuel is allowed when wheat straw pellets combusted in a fluidized bed, to maximize the effect of the additive to abate fuel ash sintering and agglomeration.[24] Moreover, analysis of the ash composition of one fuel is critical for determining both the type and amount of one additive used. Before *in situ* use, evaluation of the possible effects of one additive on the biomass ash fusion and sintering behaviors is recommended. This evaluation can be performed by performing rather simple laboratory ash sintering and fusion tests that can provide valuable information.

■ ASSOCIATED CONTENT

Supporting Information

Full documentation of the EDX element mapping of the biomass ash samples as well as corresponding ash/additive mixtures after the sintering experiments. This material is available free of charge via the Internet at http://pubs.acs.org.

AUTHOR INFORMATION

Corresponding Author

*Telephone: +47-73591602. E-mail: liang.wang@sintef.no.

Notes

The authors declare no competing financial interest.

ACKNOWLEDGMENTS

Financial support from the Research Council of Norway through the CenBio and KRAV projects is gratefully acknowledged.

REFERENCES

(1) Hupa, M. *Energy Fuels* **2011**, *26* (1), 4−14.
(2) Zevenhoven, M.; Yrjas, P.; Skrifvars, B.-J.; Hupa, M. *Energy Fuels* **2012**, *26* (10), 6366−6386.
(3) Wang, L.; Becidan, M.; Skreiberg, Ø. *Energy Fuels* **2012**, *26* (9), 5917−5929.
(4) Steenari, B. M.; Lundberg, A.; Pettersson, H.; Wilewska-Bien, M.; Andersson, D. *Energy Fuels* **2009**, *23*, 5655−5662.
(5) Lindström, E.; Larsson, S. H.; Böstrom, D.; Öhman, M. *Energy Fuels* **2010**, *24*, 3456−3461.
(6) Öhman, M.; Nyström, I.; Gilbe, C.; Boström, D.; Lindström, E.; Boman, C.; Backman, R.; Hedman, H.; Samuelsson, R.; Burvall, J.; X, S. Slag formation during combustion of biomass fuels. *Proceedings of the International Conference on Solid Biofuels*; Beijing, China, Aug 12−14, 2009.
(7) Boström, D.; Skoglund, N.; Grimm, A.; Boman, C.; Öhman, M.; Broström, M.; Backman, R. *Energy Fuels* **2011**, *26* (1), 85−93.
(8) Piotrowska, P.; Zevenhoven, M.; Hupa, M.; Giuntoli, J.; de Jong, W. *Fuel Process. Technol.* **2013**, *105*, 37−45.
(9) Skrifvars, B. J.; Hupa, M.; Backman, R.; Hiltunen, M. *Fuel* **1994**, *73* (2), 171−176.
(10) Lindstrom, E.; Sandstrom, M.; Bostrom, D.; Ohman, M. *Energy Fuels* **2007**, *21* (2), 710−717.
(11) Wang, L.; Hustad, J. E.; Grønli, M. *Energy Fuels* **2012**, *26* (9), 5905−5916.
(12) Grimm, A.; Skoglund, N.; Bostrom, D.; Ohman, M. *Energy Fuels* **2011**, *25* (3), 937−947.
(13) Wu, H.; Castro, M.; Jensen, P. A.; Frandsen, F. J.; Glarborg, P.; Dam-Johansen, K.; Rokke, M.; Lundtorp, K. *Energy Fuels* **2011**, *25* (7), 2874−2886.
(14) Wang, L.; Hustad, J. E.; Skreiberg, Ø.; Skjevrak, G.; Grønli, M. *Energy Procedia* **2012**, *20*, 20−29.
(15) Wu, H.; Glarborg, P.; Frandsen, F. J.; Dam-Johansen, K.; Jensen, P. A. *Energy Fuels* **2011**, *25* (7), 2862−2873.
(16) Steenari, B. M.; Lindqvist, O. *Biomass Bioenergy* **1998**, *14* (1), 67−76.
(17) Llorente, M. J. F.; Arocas, P. D.; Nebot, L. G.; García, J. E. C. *Fuel* **2008**, *87* (12), 2651−2658.
(18) Gilbe, C.; Öhman, M.; Lindström, E.; Boström, D.; Backman, R.; Samuelsson, R.; Burvall, J. *Energy Fuels* **2008**, *22* (5), 3536−3543.
(19) Öhman, M.; Boström, D.; Nordin, A.; Hedman, H. *Energy Fuels* **2004**, *18* (5), 1370−1376.
(20) Wang, L.; Skjevrak, G.; Hustad, J. E.; Grønli, M.; Skreiberg, Ø. *Energy Procedia* **2012**, *20*, 30−39.
(21) Zheng, Y.; Jensen, P. A.; Jensen, A. D.; Sander, B.; Junker, H. *Fuel* **2007**, *86* (7−8), 1008−1020.
(22) Li, Q. H.; Zhang, Y. G.; Meng, A. H.; Li, L.; Li, G. X. *Fuel Process. Technol.* **2013**, *107*, 107−112.
(23) Fang, X.; Jia, L. *Bioresour. Technol.* **2012**, *104*, 769−774.
(24) Skoglund, N.; Grimm, A.; Öhman, M.; Boström, D. *Energy Fuels* **2013**, *27* (10), 5725−5732.
(25) Wang, C.; Wu, Y.; Liu, Q.; Yang, H. *Fuel* **2011**, *90* (9), 2939−2944.
(26) Tobiasen, L.; Skytte, R.; Pedersen, L. S.; Pedersen, S. T.; Lindberg, M. A. *Fuel Process. Technol.* **2007**, *88* (11−12), 1108−1117.
(27) Wang, L.; Skjevrak, G.; Hustad, J. E.; Grønli, M. G. *Energy Fuels* **2011**, *25* (12), 5775−5785.
(28) Elled, A. L.; Davidsson, K. O.; Amand, L. E. *Biomass Bioenergy* **2010**, *34* (11), 1546−1554.
(29) Pettersson, A.; Zevenhoven, M.; Steenari, B.-M.; Åmand, L.-E. *Fuel* **2008**, *87* (15−16), 3183−3193.
(30) Åmand, L.-E.; Leckner, B.; Eskilsson, D.; Tullin, C. *Fuel* **2006**, *85* (10−11), 1313−1322.
(31) Knudsen, J. N.; Tobiasen, L.; Møller, H. B.; Frei, D.; Henriksen, D.; Clasusen, S. Evaluation of non-commercial additives for slagging and corrosion prevention in biomass-fired boilers. *Proceedings of the 17th European Biomass Conference and Exhibition*; Hamburg, Germany, June 29−July 3, 2007; pp 1400−1406.
(32) Pettersson, A.; Åmand, L.-E.; Steenari, B.-M. *Fuel* **2009**, *88* (9), 1758−1772.
(33) Masia, A. A. T.; Buhre, B. J. P.; Gupta, R. P.; Wall, T. F. *Fuel Process. Technol.* **2007**, *88* (11−12), 1071−1081.
(34) Knudsen, J. N.; Jensen, P. A.; Dam-Johansen, K. *Energy Fuels* **2004**, *18* (5), 1385−1399.
(35) Johansen, J. M.; Jakobsen, J. G.; Frandsen, F. J.; Glarborg, P. *Energy Fuels* **2011**, *25* (11), 4961−4971.
(36) Hall, F. P.; Insley, H. *Phase Diagrams for Ceramists*; The American Ceramic Society: Westerville, OH, 1947.
(37) Frandsen, F. J.; Novakovic, A.; van Lith, S. C.; Jensen, P. A.; Holgersen, L. B. *Energy Fuels* **2009**, *23* (7), 3423−3428.
(38) van Dyk, J. C. *Miner. Eng.* **2006**, *19* (3), 280−286.
(39) Boström, D.; Grimm, A.; Boman, C.; Bjornböm, E.; Öhman, M. *Energy Fuels* **2009**, *23*, 5184−5190.
(40) Risnes, H.; Fjellerup, J.; Henriksen, U.; Moilanen, A.; Norby, P.; Papadakis, K.; Posselt, D.; Sørensen, L. H. *Fuel* **2003**, *82* (6), 641−651.
(41) Lindström, E.; Öhman, M.; Backman, R.; Boström, D. *Energy Fuels* **2008**, *22* (4), 2216−2220.
(42) Öhman, M.; Nordin, A.; Skrifvars, B. J.; Backman, R.; Hupa, M. *Energy Fuels* **2000**, *14* (1), 169−178.
(43) De Geyter, S.; Ohman, M.; Bostrom, D.; Eriksson, M.; Nordin, A. *Energy Fuels* **2007**, *21* (5), 2663−2668.
(44) Reifenstein, A. P.; Kahraman, H.; Coin, C. D. A.; Calos, N. J.; Miller, G.; Uwins, P. *Fuel* **1999**, *78* (12), 1449−1461.